J BONE ONCOL 42 (2023) 100495

Contents lists available at ScienceDirect

Journal of Bone Oncology

journal homepage: www.elsevier.com/locate/jbo

Research Paper

Cav3.2 T-Type calcium channels downregulation attenuates bone cancer pain induced by inhibiting IGF-1/HIF-1α signaling pathway in the rat spinal cord

Qingying Liu [a,1], Zhongyuan Lu [a,1], Huan Ren [a], Lijun Fu [a], Yueliang Wang [a], Huilian Bu [a], Minyu Ma [a], Letian Ma [a], Chen Huang [a], Jian Wang [a,b], Weidong Zang [b,c,*], Jing Cao [b,c,*], Xiaochong Fan [a,*]

[a] Department of Pain Medicine, The First Affiliated Hospital of Zhengzhou University, Zhengzhou, Henan 450052, China
[b] Department of Human Anatomy, School of Basic Medical Sciences, Zhengzhou University, Zhengzhou, Henan Province 450001, China
[c] Institute of Neuroscience, Zhengzhou University, Zhengzhou, Henan Province 450001, China

HIGHLIGHTS

- Cav3.2 T-type calcium channel is upregulated after bone cancer-induced pain.
- Specific knockdown of Cav3.2 channel attenuates mechanical and thermal nociceptive hyperalgesia in bone cancer pain rats.
- The role of Cav3.2 T-type calcium channel in alleviating pain hypersensitivity is achieved by inhibiting the IGF-1/HIF-1α signaling pathway.
- We propose a positive regulation of Cav3.2 by HIF-1α at the transcriptional level.
- We are the first to study the mechanism of Cav3.2 T-type calcium channel in bone cancer pain.

ARTICLE INFO

Keywords:
Bone cancer pain
Cav3.2 T-type calcium channels
IGF-1
HIF-1α
Spinal dorsal horn

ABSTRACT

Background: Bone cancer pain (BCP) is one of the most ubiquitous and refractory symptoms of cancer patients that needs to be urgently addressed. Substantial studies have revealed the pivotal role of Cav3.2 T-type calcium channels in chronic pain, however, its involvement in BCP and the specific molecular mechanism have not been fully elucidated.

Methods: The expression levels of Cav3.2, insulin-like growth factor 1(IGF-1), IGF-1 receptor (IGF-1R) and hypoxia-inducible factor-1α (HIF-1α) were detected by Western blot in tissues and cells. X-ray and Micro CT used to detect bone destruction in rats. Immunofluorescence was used to detect protein expression and spatial location in the spinal dorsal horn. Electrophoretic mobility shift assay used to verify the interaction between HIF-1α and Cav3.2.

Results: The results showed that the expression of Cav3.2 channel was upregulated and blockade of this channel alleviated mechanical allodynia and thermal hyperalgesia in BCP rats. Additionally, inhibition of IGF-1/IGF-1R signaling not only reversed the BCP-induced upregulation of Cav3.2 and HIF-1α, but also decreased nociceptive hypersensitivity in BCP rats. Inhibition of IGF-1 increased Cav3.2 expression levels, which were abolished by pretreatment with HIF-1α siRNA in PC12 cells. Furthermore, nuclear HIF-1α bound to the promoter of Cav3.2 to regulate the Cav3.2 transcription level, and knockdown of HIF-1α suppresses the IGF-1-induced upregulation of Cav3.2 and pain behaviors in rats with BCP.

Conclusion: These findings suggest that spinal Cav3.2 T-type calcium channels play a central role during the development of bone cancer pain in rats via regulation of the IGF-1/IGF-1R/HIF-1α pathway.

* Corresponding authors at: Department of Pain Medicine, The First Affiliated Hospital of Zhengzhou University, No. 1 East Construction Road, Erqi District, Zhengzhou, Henan 450052, China (Xiaochong Fan). Department of Human Anatomy, Zhengzhou University, 100 Science Avenue, Zhengzhou 450001, China (Jing Cao and Weidong Zang).

E-mail addresses: zwd@zzu.edu.cn (W. Zang), caojing@zzu.edu.cn (J. Cao), fccfxc@zzu.edu.cn (X. Fan).

[1] These authors contributed equally to this work.

https://doi.org/10.1016/j.jbo.2023.100495
Received 21 March 2023; Received in revised form 20 July 2023; Accepted 24 July 2023
Available online 1 August 2023

1. Introduction

Bone cancer pain (BCP) is one of the most common symptoms experienced by patients with bone metastases, notably those with advanced breast, lung, and prostate cancer [1], and lacks effective therapeutic approaches. In the pain pathway, the persistent neural signals delivered from bone induce structural and functional changes to the spinal cord dorsal horn, and this neuroplasticity promotes the development of central hyperexcitability to facilitate BCP [2,3]. These changes are characterized by the number and functional ion channels in the affected sensory neurons, wherein the unique low-voltage activated (LVA) T-type calcium channels suggest that they are major regulators in nociceptive transmission [4]. Most of these studies suggested that spinal Cav3.2 T-type calcium channels showed potent analgesic effects in various types of acute or chronic pain [5,6], while until recently, the exact role of Cav3.2 T-type calcium channels in cancer pain mechanisms was little known. Based on observations that the vital effect of Cav3.2 T-type channels on cancer growth progression and proliferation [7], and our preliminary results showed that Cav3.2 expression was increased in BCP rats. We hypothesized that the Cav3.2 channel may be a novel therapeutic target not only for cancer but also for cancer-induced pain management treatment.

Cav3.2 T-type calcium channels have been reported to be regulated by insulin-like growth factor 1 (IGF-1) through stimulation of IGF-1 receptor (IGF-1R) [8]. IGF-1 is a polypeptide growth factor that plays a vital role in cell progression, differentiation, antioxidant activity and tumorigenesis [9]. Previous work found that IGF-1 upregulated the function of transient receptor potential vanilloid 1 (TRPV1) in the nerves of bone cancer pain rats [10]. Activation of TRPV1 triggers a protective pain status rely on the USP5/Cav3.2 interactions after nerve injury [11]. However, the effects and molecular modulation mechanisms of IGF-1 on Cav3.2 T-type calcium channels in bone cancer pain have not been elucidated.

Hypoxia-inducible factor-1α (HIF-1α) is a highly specific nuclear transcription factor that plays an important role in cellular perception and adaptation to changes in oxygen partial pressure in the internal environment [12]. Studies have shown that IGF-1/IGF-1R signaling stimulates HIF-1α expression via the activation of VEGF in breast tumor microenvironment [13], and inhibiting HIF-1α/VEGF axis alleviates nociception in animals with neuropathic and cancerous pain [14,15]. Furthermore, HIF-1α controls the transcription of multiple calcium-regulated factors, leading to remodeling of the calcium signaling pathway in a variety of cancer types, including breast, liver, colon, and glioma [16], and chronic intermittent hypoxia activates HIF-1α to promote Cav3.2 translocation to the cytosol and increase the T-current [17]. This evidence raises the possibility that upregulation of Cav3.2 T-type calcium channels in the spinal cord contributes to the development of BCP mediated by the IGF-1/IGF-1R/HIF-1α signaling cascade. To test this hypothesis, we examined the influence of Cav3.2 channels on behavioral changes in chronic bone cancer pain induced by intratibial inoculation of mammary rat metastatic tumor cells and examined the potential molecular regulatory mechanism using corresponding drug interventions.

2. Materials and methods

2.1. Animals

Female Sprague-Dawley (SD) rats weighing 150 to 180 g at the start of experiments were purchased from the laboratory animal center of Zhengzhou University. Animals were housed in a standard 12 h reversed light/dark cycle at 22 to 25 ℃ with free access to food and water. All experimental procedures for animals were carried out according to the relevant guidelines and regulations of the International Association for the Study of Pain and were approved by the Animal Protection and Use Committee of Zhengzhou University.

2.2. Drugs and administration

Selective Cav3.2 siRNA (sc-61870, Santa Cruz Biotechnology), selective HIF-1α siRNA (sc-45919, Santa Cruz Biotechnology) and control siRNA (sc-37007, Santa Cruz Biotechnology) were purchased. These siRNAs were dissolved in RNase-free water at 1 μg/μl as a stock solution and mixed with the transfection reagent (sc29528, Santa Cruz Biotechnology) before injection, following the manufacturer's instruction.

JB-1 (147819-32-7, Sigma-Aldrich), an antagonist of IGF-1R, was dissolved in sterile normal saline (NS) to 10 μg/μl as stock solution. Recombinant IGF-1 (abs01076, Absin Bioscience) were dissolved at 1 mg/ml in 0.01 M phosphate buffered saline (PBS) and stored at −20 °C.

2.3. Cell culture

The Mammary rat metastasis tumor cells (MRMT-1) were purchased from Guandao Bioengineering (Shanghai, China). Cells were cultured with RPMI-1640 medium (Gibco Company), 10% fetal bovine serum (FBS) (Gibco Company) and 1% penicillin/streptomycin with constant temperature of 37° C and a humidified atmosphere of 5% CO_2. On the day of modeling, cells were released by exposure to 0.25% trypsin (Gibco Company) and collected by centrifugation at 1000 rpm for 5 min. MRMT-1cells were suspended in Dulbecco's phosphate buffered saline (DPBS) to final concentration of 1×10^7 cells/ml and kept on ice. Live cells were counted by trypan blue staining. The PC12 (rat pheochromocytoma) cell line was purchased from Procell (Wuhan, China) and cultured in highly differentiated PC12 cell medium (Procell) at 37° C in a humidified incubator of 5 % CO_2. Cells were seeded in a 6-well plate with $0.25 - 1 \times 10^6$ cells per well until the microscopic cell area was approximately 70%, Dulbecco's modified Eagle medium (DMEM) (HyClone) was replaced and IGF-1 recombinant protein was added at a concentration of 50 ng/ml [10] at 12, 24 and 48 h, respectively. All cell lines used in our research were authenticated using cell species test before use.

2.4. Transient transfection of siRNA

PC12 cells were inoculated in a 6-well tissue culture plate and siRNAs were transfected until the area of the microscope cells reached presumably 70%. According to the suggestion of the transfection reagent manufacturer, solution A was obtained by diluting 5 μl siRNA into 100 μl DMEM, and solution B was obtained by diluting 5 μl siRNA into 100 μl DMEM. Solution A and solution B were mixed and incubated at room temperature for 20 min. The transfection mixture were covered on the washed PC12 cells and incubated in a 37° C incubator for 6 h. After 2 – 4 days, cells were collected for analysis.

2.5. Bone cancer-induced pain model

An intra-tibial bone cavity administration of MRMT-1 rat mammary gland carcinoma cells was used to generate bone cancer-induced pain [18]. Rats were anesthetized with isoflurane (induction 5%, maintenance 1.5 – 2%, at 2 L/min O_2). Under aseptic condition, a small incision was made in the scraped and sterilized area of anterior medial surface of the right tibia. The tibia was exposed and a hole was drilled at the site of the proximal intramedullary cavity with a 23-gauge needle. Using a 10 μl Hamilton syringe, a total of 5 μl suspension containing 1×10^7 cancer cells or heat-killed cells was injected slowly into the cavity. After injection, the site was immediately sealed with sterile bone wax and the incision wound was layered sutured. In this article, bone cancer pain refers to MRMT-1 induced bone cancer pain.

2.6. Behavioral tests

Each animal was acclimated to a Plexiglas cube environment for 30 min per day for 3 consecutive days before testing. Mechanical and

thermal pain thresholds were measured while the animals stayed calm and awake. For mechanical allodynia, 50% paw withdrawal thresholds (PWTs) were measured using the up-down method [19] and as previously described [6,20]. Eight von Frey filaments (North Coast, Gilroy, CA) in logarithmic increments of force (0.69, 1.20, 2.04, 3.63, 5.50, 8.51, 15.14 and 26 g) were used to stimulate the hind paws. Each trial started with a von Frey force of 3.63 g delivered perpendicularly to the plantar surface of the left hind-paw. An abrupt withdrawal of the foot during stimulation or immediately after the removal of the filament was recorded as a positive response. Once a positive or negative response was evoked, the next weaker or stronger filament was applied. The test was terminated when a negative reaction was used with 26.0 g stimulation or 3 stimuli after the first positive response. The 50% PWT was calculated using the following formula: 50% PWT = $10^{(X+kd)}/10^4$, where X is the value of the final von Frey filament used (in log units), k is a value measured from the pattern of positive/negative responses, and d is the average increment (in log units) between the von Frey hairs.

For the thermal nociceptive response, paw withdrawal latencies (PWLs) were measured as described previously [21,22]. The thermal stimulator power of a heat flux radiometer (Ugo Basile, Italy) was adjusted to the basal PWLs at 10 to 12 s with a cutoff time of 15 s to avoid tissue damage. PWLs were recorded 3 times at minimal 5-minute intervals for each trial and the average value was used to represent the thermal pain threshold of the rat. All behavioral tests were performed blind.

2.7. Intrathecal catheterization and drug delivery

Implantation of intrathecal catheter was performed as described previously [23]. Rats were anesthetized with isoflurane (induction 5%, maintenance 1.5 – 2%, in 2 L/min O_2). In the subarachnoid space, a PE-10 catheter was placed between the lumbar vertebra 4 and 5 to reach the lumbar enlargement level through a guide cannula. The outer the catheter was plugged and fixed on the skin between the rat ears. Ras were allowed to recover for 5 days prior to further experimental manipulations, and any animals showing motor impairment after catheter implantation were excluded.

We used intrathecal injection of siRNA specific targeted to Cav3.2 and HIF-1α to examine their effects on BCP rats. The siRNAs were diluted with the transfection reagent to a final concentration of 2 ug/10 μl, and were injected intrathecally into rats in a volume of 10 μl, followed by 10 μl of saline for flushing. In the rat that received BCP, Cav3.2 siRNA was administered per day on postoperative days 7, 8, 9 and postoperative days 14, 15, 16, respectively. Meanwhile, HIF-1α siRNA was injected with the same dose (2 ug/10 μl), but on postoperative days 7, 8, and 9 after the establishment of BCP. To verify the regulatory effect of IGF-1 on Cav3.2 in BCP rats, the drug JB-1 (an antagonist of IGF-1R, 10 ug/10 μl) was administered intrathecally daily from day 14 to day 16 after BCP. An equal volume of scrambled siRNA or saline was administered as a control.

2.8. Western blot analysis

2.8.1. Total protein preparation

Animals were deeply anesthetized with 1% pentobarbital sodium (0.1 g/kg, i.p.) and the ipsilateral spinal cord in the lumbar enlargement site was rapidly separated and homogenized in ice-cold lysis buffer containing 50 mM Tris-HCl (pH 7.4), 150 mM NaCl, 1% NP-40, 0.1% SDS, 1 mM phenylmethylsulfonyl fluoride and protease phosphatase inhibitor (Solarbio Company, China). After being kept on ice for 1 h, the lysates were centrifuged at 12,000 rpm for 15 min at 4 °C and the supernatants mixing with loading buffer were denatured at 95 °C for 5 min. The protein concentrations were measured using a bicinchoninic acid (BCA) kit (Pierce Biotechnology Inc.).

2.8.2. Nucleoprotein preparation

The nucleoprotein samples were prepared following the protocol as in our lab [24]. Briefly, the lumbar enlargement site of the ipsilateral spinal cord tissues were homogenized in lysis buffer A (10 mM Tris, 1 mM PMSF, 5 mM $MgCl_2$, 5 mM EGTA, 1 mM DTT, 100 mM NP-40, 40 mM leupeptin, and 250 mM sucrose), and kept on ice for 30 min before centrifugating at 1000 × g for 15 min at 4 °C. Sediments were mixed with lysis buffer B (9.25 mM Tris, 150 mM 10% SDS, 1 mM Triton X-100) to sonicate and incubated on ice for 30 min. Next, samples were centrifuged at 1000 × g for 15 min at 4 °C and the supernatants were collected for Western blot assay.

2.8.3. Western blot

According to a standard protocol, an equal amount (40 μg) of protein was separated from each sample on 8% – 12% SDS-PAGE and transferred to the polyvinylidene fluoride membrane (Merck Millipore). The blots were blocked in a solution of 5% non-fat milk with TBST (20 mM Tris-HCl, pH 7.6, 150 mM NaCl, 0.05% Tween 20) for 1 h at room temperature and incubated with one of the following primary antibodies at 4 °C overnight: rabbit anti-Cav3.2 (1: 200, ACC-025, Alomone Labs), rabbit anti-IGF-1 (1: 1000, 28530-1-AP, Proteintech), rabbit anti-IGF-1R β (1:1000, 3027S, Cell Signaling Technology), rabbit anti-HIF-1α (1: 2000, 20960-1-AP, Proteintech), rabbit anti-β-tubulin (1: 1000, ab179513, Abcam), or rabbit anti- Histone-H3 (1: 3000, 17168-1-AP, Proteintech). Subsequently, after washing with TBST 3 times (5 min each time), membranes were incubated with horseradish peroxidase-conjugated goat anti-rabbit secondary antibody (1:10000, A21020, abbkine) for 1 h at room temperature. Finally, the blots were detected using ECL reagents and visualized by a ChemiDoc MP System molecular imager (Bio-Rad). The films were analyzed using Quantity One software. Nuclear protein bands were normalized to Histone-H3 and β-tubulin was served as the loading control for total fractions.

2.9. Immunohistochemistry

Under anesthesia with 1% pentobarbital sodium (0.1 g/kg, i.p.), rats were perfused intracardially with warm normal saline followed by cold 4% paraformaldehyde (PFA) in 0.1 M phosphate buffer (PB). The whole spinal cord in L4 – L5 segments was rapidly dissected and post-fixed in 4% PFA for 6 h, then cryoprotected by incubation of PB with 20% and 30% sucrose solutions at 4° C in turn. 25 μm sections were sliced horizontally using a cryostat microtome (CM1900, Leica). Based on a standard protocol, free-floating sections were washed in PBS, blocked in 10% normal goat serum with 0.3% Triton X-100 in PBS for 1 h at room temperature, and incubated with one of the following primary antibodies: rabbit anti-Cav3.2 antibody (1: 200, ACC-025, Alomone Labs), mouse anti-IGF-1R β antibody (1:50, sc-390130, Santa Cruz Biotechnology), mouse anti-ionized calcium binding adaptor 1 (IBA1, a microglia marker, 1: 200, ab283319, Abcam), mouse anti-glial fibrillary acidic protein (GFAP, an astrocyte marker, 1: 200, ab4648, Abcam) or mouse anti-neuronal specific nuclear protein (NeuN, a neuronal marker, 1: 200, 66836-1-Ig, Proteintech) in 1% bovine serum albumin (BSA) with 0.3% Triton X-100 at 4 °C for 24 h. Sections were then washed in PBS and incubated with one of the following secondary antibodies at room temperature for 2 h: Alexa Fluor 488 conjugated goat anti-rabbit IgG (1: 100, 111-545-003, Jackson ImmunoResearch Laboratories), Alexa Fluor 568 conjugated goat anti-mouse IgG (1: 200, A-11004, Thermo Fisher Scientific), rinsed in PBS, then dried and covered with anti-fade mounting medium. Images were taken with a fluorescence microscope (BX53, Olympus). Schematic representation of the spinal dorsal horn superficial layer, a central portal for pain afferents and local information processing. For quantification, 4 – 6 non-consecutive sections of each of 4 rats per group were imaged and counted using Image J software. Only cells with clear nuclear morphology were subjected to quantification analysis. The sections were counterstained with DAPI to label cell nuclei.

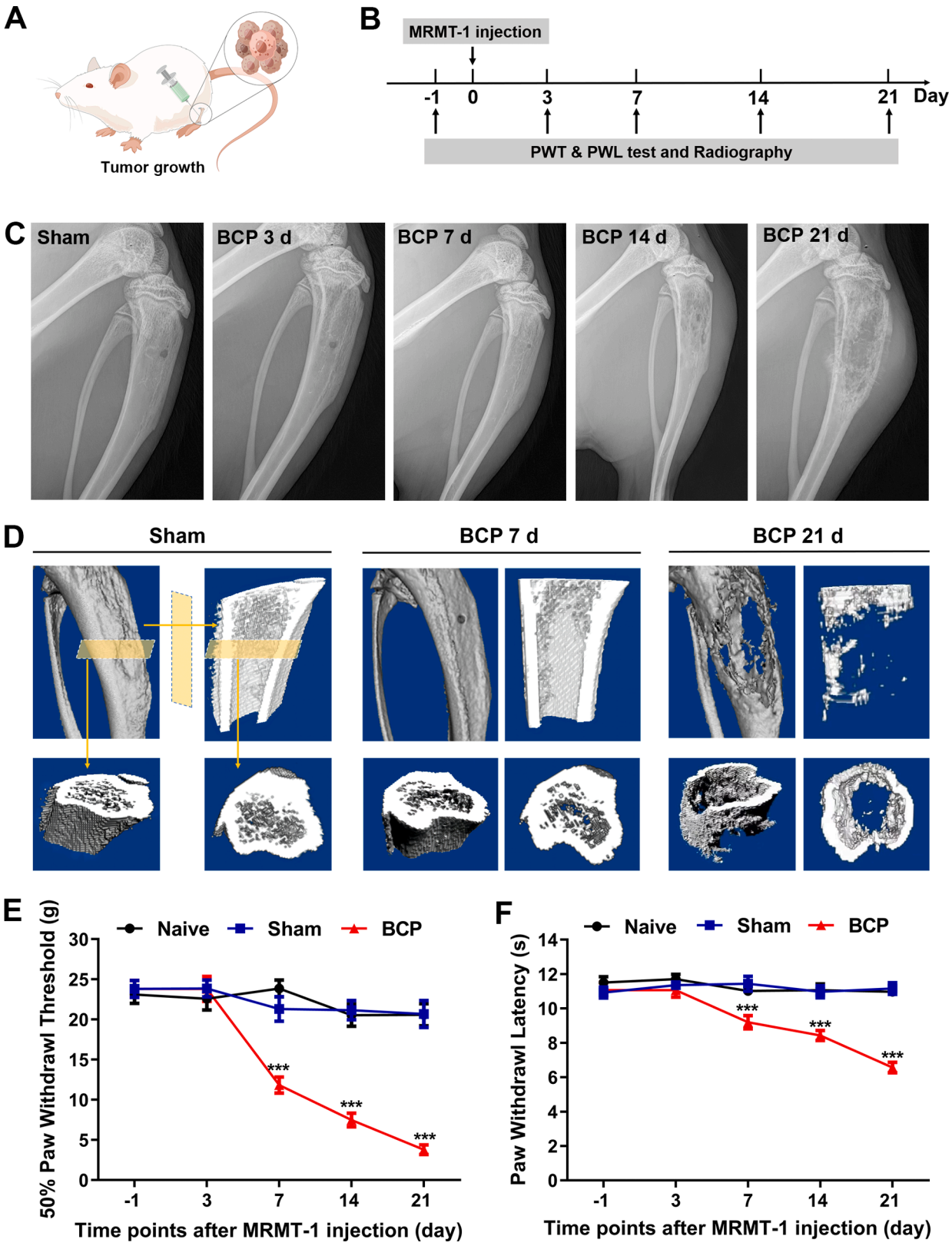

Fig. 1. Establishment of the MRMT-1-induced BCP rat model. (A) A rat model of BCP was established by intratibial injection of MRMT-1 cells into SD rats. (B) Experimental diagram showing the timeline of behavior and radiography tests in the BCP model. (C) Representative radiographs of rat ipsilateral tibia in sham operation and days 3, 7, 14, 21 after MRMT-1 inoculation. Progressive cancer-induced osteolytic bone destruction was reflected during the development of BCP, especially on day 21 after tumor inoculation. (D) Example micro-CT reconstructions of rat tibia in sham operation, an early (day 7) and a late (day 21) cancer phase. Upper: Coronal plane of the ipsilateral tibia; lower: Horizontal plane of the ipsilateral tibia. Note increased lesions in the trabecular and cortical bone in rats 21 days after tumor implantation. (E, F) Mechanical allodynia (E) and thermal hyperalgesia (F) developed on the 7 days and lasted at least 21 days after BCP. There was no difference between the naive group and the sham group in mechanical allodynia and thermal hyperalgesia. n = 8 per group. ***$p < 0.001$, two-way ANOVA followed by Bonferroni's post hoc test.

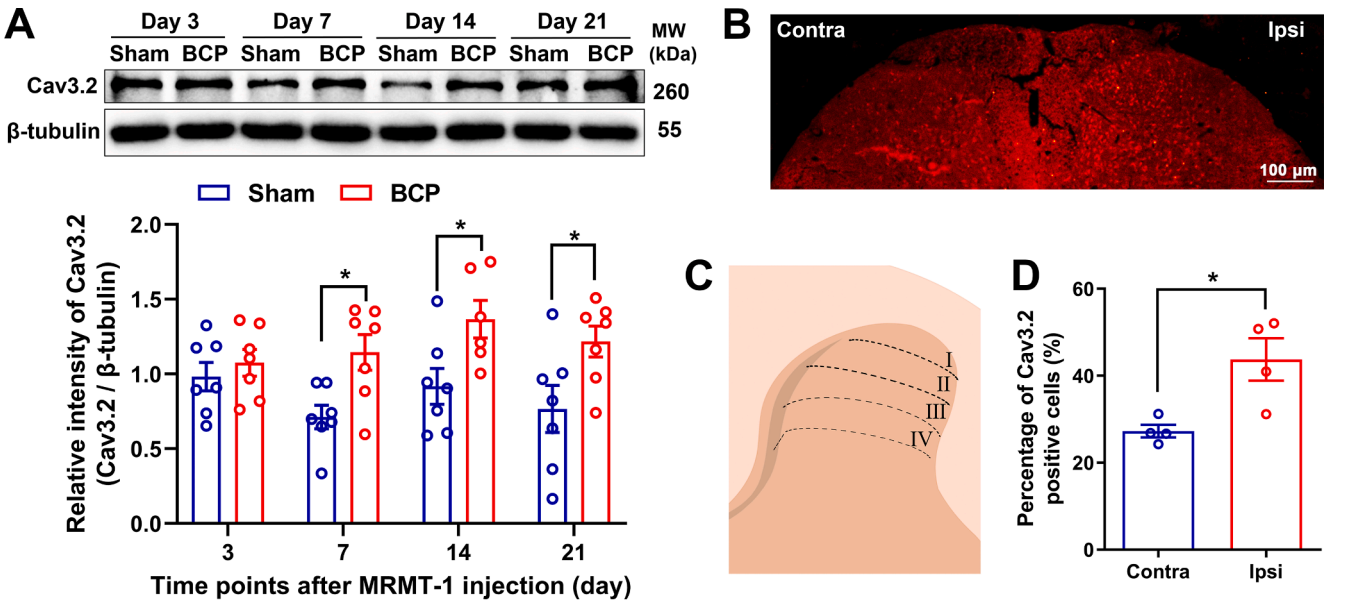

Fig. 2. Expression of Cav3.2 T-type calcium channels is increased in BCP rats. (A) The expression of Cav3.2 protein increased from day 7 to day 21 in BCP rats compared to sham operation rats. Upper: representative image of Western blot bands in ipsilateral side of the lumbar enlargement lysates; lower: statistical analysis of protein expression. n = 7. $*p < 0.05$, two-way ANOVA with Bonferroni's *post hoc* test. (B) Representative images of immunohistological staining showed an increase in Cav3.2 positive cells in the superficial layer of the ipsilateral (Ipsi), but not contralateral (Contra) dorsal horn on day 14 in BCP rats. (C) Schematic representation of the superficial layer in the spinal dorsal horn. (D) Quantitative analysis revealed a significant increase in Cav3.2 positive staining cells in the dorsal horn (laminae I-IV; as indicated in C) in BCP rats. Scale bar = 100 μm. n = 4. $*p < 0.05$, $***p < 0.001$, unpaired *t* test.

2.10. Electrophoretic mobility shift assay (EMSA)

To study the interaction of the Cav3.2 DNA with HIF-1α nuclear protein, we used the EMSA kit (20148, Thermo Fisher Scientific) for this assay according to manufacturer's protocol. Double-stranded oligonucleotides with the primers 5′-GAAGGGCACGCGCCTCGCGG-3′ and 5′-CCGCGAGGCGCGTGCCCTTC-3′ were used as probe and biotin-labeled. Nuclear extracts were prepared using the nuclear and cytoplasmic protein extraction kit (P0028, Beyotime). Briefly, the respective biotin-labeled oligonucleotides were added to a 20 μl reaction mix containing 2 μg of nuclear extracts, recommended volumes of DNA binding buffer, poly (dI-dC), 50% glycerol, 1% NP-40, 100 mM $MgCl_2$ and 200 mM EDTA. For the competition assay, additional unlabeled or mutated oligonucleotides were added. The DNA-nuclear protein complexes were then separated on a 5.5% Native-PAGE by electrophoresis and transferred onto a polyvinylidene fluoride membrane. Images were detected using the Bio-Rad ChemiDoc MP system.

The sequence of the mutated probe was 5′-GAAGGTAGATATACTCGCGG-3′ and 5′-CCGCGAGTATATCTACCTTC-3′, the sequence of the cold probe was 5′-GAAGGGCACGCGCCTCGCGG-3′ and 5′-CCGCGAGGCGCGTGCCCTTC-3′.

2.11. X-ray radiography

Rats were anesthetized with isoflurane (5% for induction, 3% for maintenance, 2 L/min O_2) and placed on a X-Viewer apparatus. Radiological detection of tibia was performed to determine bone destruction.

2.12. Microcomputed tomography (Micro-CT)

MicroCT analysis was performed on rats using a Micro CT-NEMO scanner (NMC-200, PINGSENG Healthcare). For reconstruction, CTAn software (version 1.16.9.0) was used. And three-dimensional model analysis was performed using CT vox software (version 3.3).

2.13. Statistical analysis

All data were presented as mean ± standard error (SEM) and analyzed using GraphPad Prism 8.0 software. Statistical analysis of two groups was performed using Student's t tests with unpaired two-tailed scores, comparisons between groups were performed using one-way or two-way analysis of variance (ANOVA) followed by Bonferroni post hoc tests. Differences with $p < 0.05$ were considered statistically significant.

3. Results

3.1. Intratibial tumor cell injection induces bone destruction and nociceptive hypersensitivity

The MRMT-1 cells were injected into the tibial bone to induce BCP in rats (Fig. 1A). The model was validated by tibial radiographs and behavioral analysis at −1, 3, 7, 14, and 21 days after surgery (Fig. 1B). X-ray showed that bone destruction gradually increased with the progression of MRMT-1 inoculation, and definite regional bone destruction was detected on day 14 after tumor implantation, followed by the development of osteolytic bone lesions on postoperative day 21 (Fig. 1C). We also selected two different time points, early phase day 7 and late phase day 21 after the operation, to measure the bone density of cancer-bearing tibias using micro-CT and reconstruction techniques. The images showed destruction of the trabecular and cortical bone around the tibial part at the later stage of the development of BCP compared to those of the sham group (Fig. 1D).

To evaluate the effects of tumor inoculation on pain hypersensitivity in rats, von Frey and radiant heat measurements were used to detect changes in mechanical and thermal sensitivity on days 3, 7, 14 and 21 after the BCP operation. In rats receiving tumor cell injection, the quantitative value of 50% PWTs and PWLs decreased significantly on day 7 and was maintained until day 21 postoperation, and the 50% PWTs and PWLs did not show significant differences between the naive group and the sham group (Fig. 1E, F).

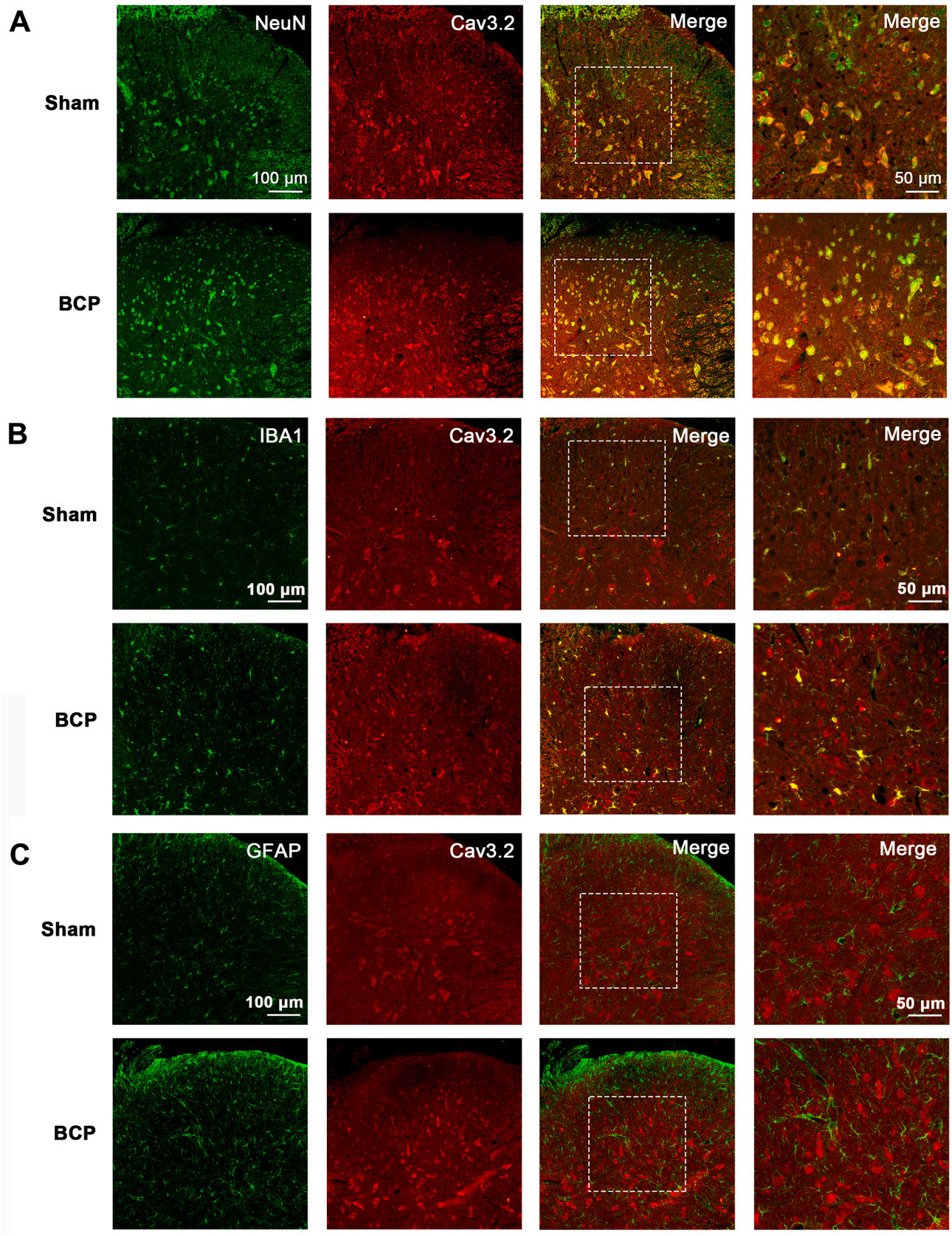

Fig. 3. Increased distribution of Cav3.2 in the spinal cord following BCP. (A-C) Representative immunohistochemical staining showed that Cav3.2 was expressed primarily in neurons (A) and partially in microglia (B), lacked colocalization with astrocytes (C) in the dorsal horn of BCP rats.

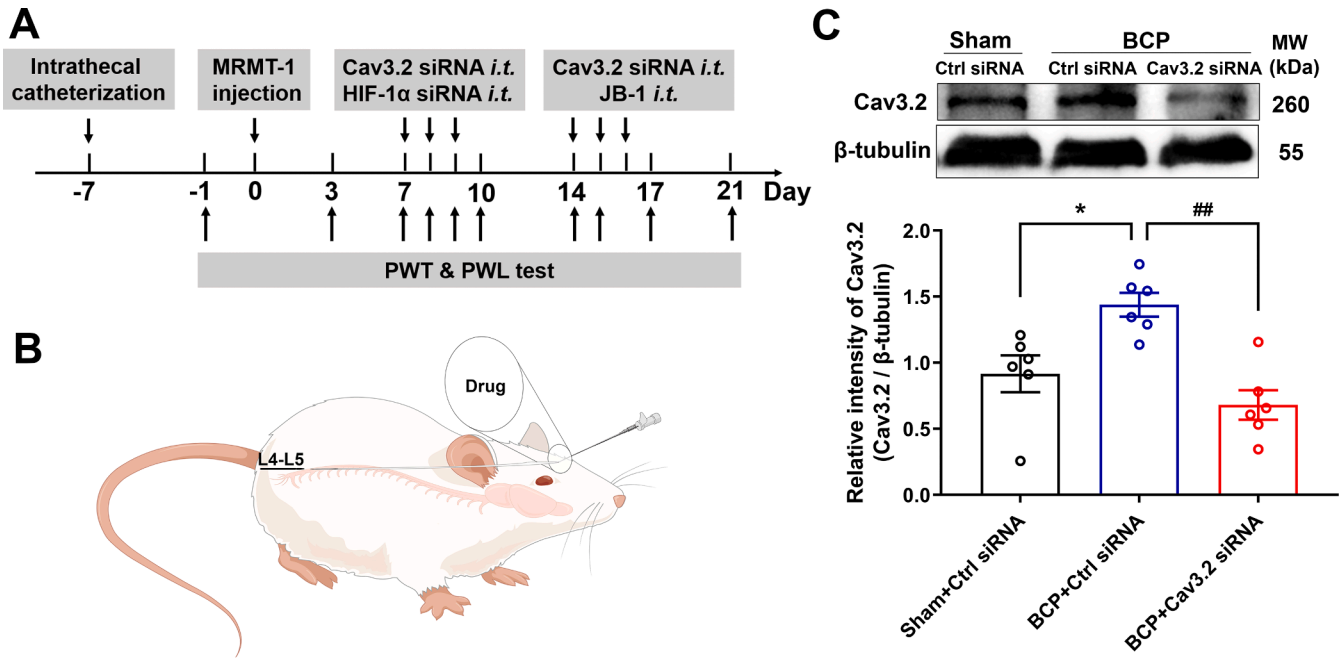

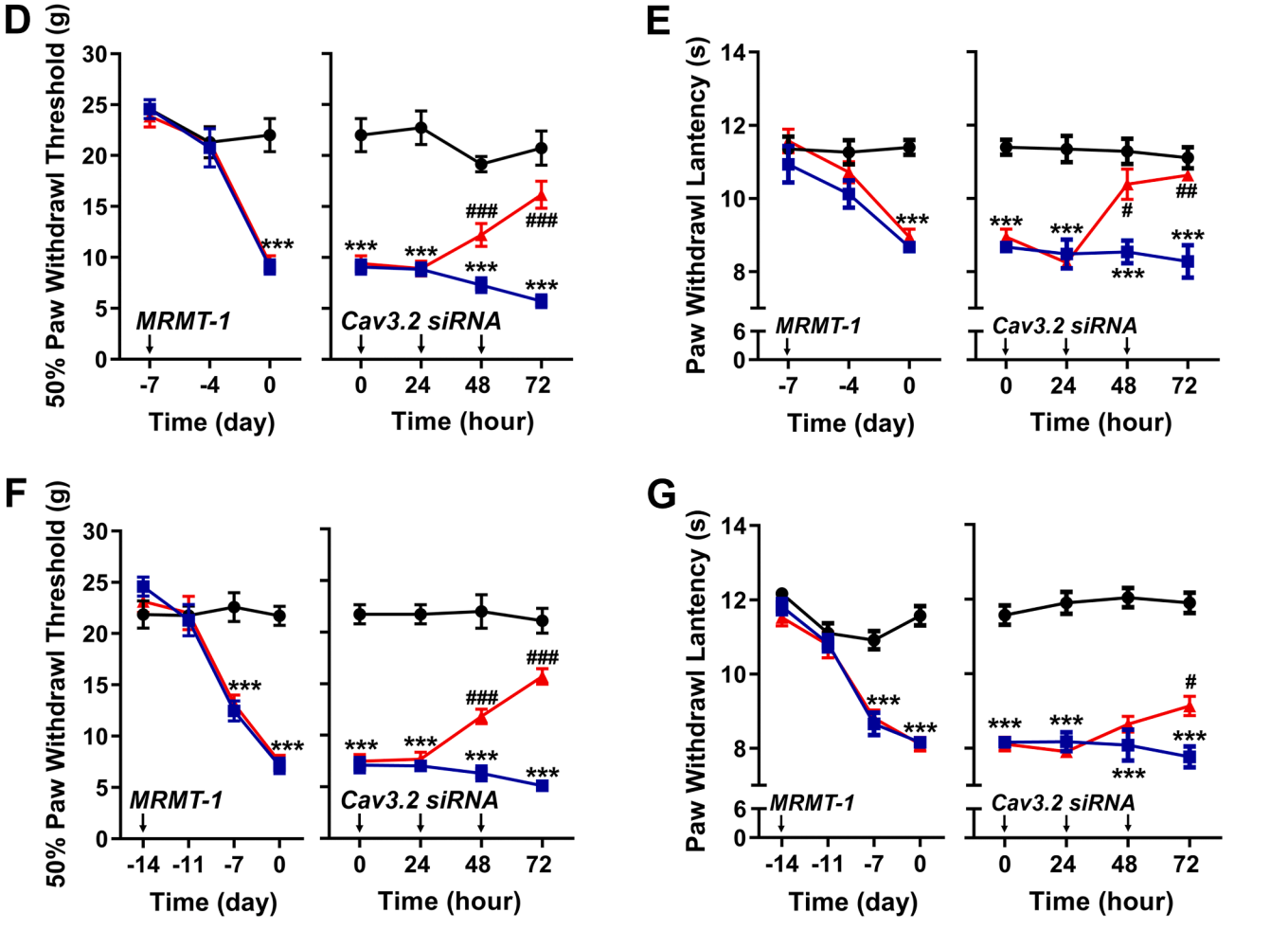

(caption on next page)

Fig. 4. Knockdown of Cav3.2 attenuates mechanical allodynia and thermal hyperalgesia induced by BCP. (A) Brief timeline of the experimental diagram in the MRMT-1-induced BCP model. (B) Schematic diagram of intrathecal administration in rats. (C) Pretreatment with Cav3.2 siRNA reversed the BCP-induced increase in Cav3.2. Upper: representative image of Western blot bands in ipsilateral side of the lumbar enlargement lysates; lower: statistical analysis of protein expression. n = 6. $^{*}p < 0.05$, BCP + Ctrl siRNA *vs.* Sham + Ctrl siRNA; $^{\#\#}p < 0.01$, BCP + Cav3.2 siRNA *vs.* BCP + Ctrl siRNA, unpaired *t* test. (D-G) Three consecutive days of intrathecal application of Cav3.2 siRNA attenuated mechanical allodynia and thermal hyperalgesia 7 days (D and E) and 14 days (F and G) after BCP. n = 8. $^{***}p < 0.001$, BCP + Ctrl siRNA *vs.* Sham + Ctrl siRNA; $^{\#}p < 0.05$, $^{\#\#}p < 0.01$, $^{\#\#\#}p < 0.001$, BCP + Cav3.2 siRNA *vs.* BCP + Ctrl siRNA, two-way ANOVA with Bonferroni's *post hoc* test.

3.2. Expression of Cav3.2 T-type calcium channels is upregulated and primarily localized in spinal dorsal horn neurons during bone cancer-induced pain

To determine the role of Cav3.2 during the development of BCP, we first examined Cav3.2 alteration using a Western blot assay in the dorsal horn of the spinal cord at 3, 7, 14 and 21 days after BCP. The results showed that Cav3.2 protein increased significantly from day 7 to day 21 in BCP rats compared to sham-operated rats (Fig. 2A). To visualize Cav3.2 expression, we next selected 14 days after the operation as a representative time point to examine the cellular localization of Cav3.2 in the spinal cord using immunohistochemical staining. Our results showed an obvious increase in Cav3.2-positive cells in the ipsilateral dorsal horn compared to the contralateral side (Fig. 2B-D).

We further identified the cell subtypes of increased Cav3.2 channel in the ipsilateral dorsal horn using double immunofluorescent staining of Cav3.2 with NeuN, IBA1, or GFAP. The results showed that this increased expression of Cav3.2 was colocalized mainly with neurons (Fig. 3A) and slight microglia (Fig. 3B) but not in astrocytes (Fig. 3C) in the spinal cord dorsal horn. These results demonstrate that the Cav3.2 channel is upregulated in the spinal cord during the development of BCP and suggest that neurons may be responsible for BCP-induced Cav3.2 expression.

3.3. Knockdown of the Cav3.2 calcium channels attenuates pain behaviors in rats with BCP

To further validate whether the Cav3.2 channels are involved in the development of BCP, we used an intrathecal injection approach and a genetic siRNA specifically targeting the Cav3.2 in bone cancer rats (Fig. 4A, B). First, repeated intrathecal injection of Cav3.2 siRNA (2 μg/10 μl, once per day from day 7 to day 9 after the operation) significantly inhibited Cav3.2 expression in BCP rats compared to the control siRNA treatment group (Fig. 4C). Behaviorally, spinal administration of Cav3.2 siRNA dramatically attenuated BCP-induced mechanical allodynia (Fig. 4D) and thermal hyperalgesia (Fig. 4E) within 48 h and lasted up to 72 h longer than that of the control group. Furthermore, we examined the effects of consecutive administration of Cav3.2 siRNA on pain behaviors on postoperative days 14, 15 and 16 with the same dose. Similarly, Cav3.2 siRNA also showed apparent analgesic effects on mechanical allodynia (Fig. 4F) and thermal hyperalgesia (Fig. 4G) 48 to 72 h after injection. These results highlighted the crucial roles of Cav3.2 T-type calcium channels in the early and late stages of BCP.

3.4. IGF-1 and IGF-1R are increased in the spinal cord of BCP rats, and inhibition of IGF-1/IGF-1R signaling reduces the IGF-1-induced upregulation of Cav3.2 and attenuates pain hypersensitivity in BCP rats

To investigate the regulatory effect of IGF-1 on Cav3.2 levels, we first examined the expression changes in IGF-1 and its receptor IGF-1R in the spinal cord of rats with BCP. Western blot results showed that the expression of IGF-1 was significantly increased from day 14 to day 21 in BCP rats compared to sham rats (Fig. 5A), and IGF-1R increased significantly from day 3 to day 21 in BCP rats in contrast to sham rats (Fig. 5B). In addition, the double immunofluorescence staining showed that IGF-1R colocalized with Cav3.2 in both sham and BCP rats, and there was an obvious increase in the colocalization of IGF-1R and Cav3.2 in the superficial layer of the spinal dorsal horn 14 days after BCP compared with the sham group (Fig. 5C, D). This result provided a morphological basis for the action of IGF-1 on Cav3.2.

We next determined whether the increased IGF-1 could induce upregulation of Cav3.2 in vitro. After incubation with IGF-1 (50 ng/ml) 48 and 72 h in PC12 cells, the expression of Cav3.2 was increased significantly compared to the PBS treatment group (Fig. 5E). To further validate whether IGF-1/IGF-1R signaling affects the development of BCP through activation of the Cav3.2 channel, JB-1, an antagonist of IGF-1R, was used. JB-1 is an IGF-1 peptide analog that specifically acts on IGF-1R to inhibit IGF-1-induced activities, including cellular proliferation and neural development [25]. The results showed that intrathecal application of JB-1 (10 μg/10 μl) significantly prevented IGF-1-stimulated Cav3.2 accumulation in BCP rats (Fig. 5F). Next, we detected the contribution of IGF-1 in vivo. JB-1 was injected intrathecally for 3 consecutive days from days 14 to 16 after inoculation of MRMT-1 cells when IGF-1 expression was evident. Likewise, JB-1 significantly attenuated the mechanical (Fig. 5G) and thermal sensitivity (Fig. 5H) induced by BCP from 1 h and was maintained until 72 h postinjection. These results indicate that IGF-1/IGF-1R signaling contributes to the upregulation of Cav3.2 T-type calcium channels during the development of BCP.

3.5. Inhibition of IGF-1/IGF-1R signaling reduces the expression of HIF-1α, and knockdown of HIF-1α suppresses the IGF-1-induced upregulation of Cav3.2 in rats with BCP

We continued to examine the downstream target on which the increased IGF-1/IGF-1R exerts its effect on the development of BCP. Here, we centered on HIF-1α, a highly specific nuclear transcription factor that can be regulated by IGF-1 [26]and is well reported to be involved in the pathogenesis of diverse types of cancer [27]. First, the expression of the total HIF-1α protein increased markedly on day 21 in BCP rats compared to sham rats (Supplementary Fig. S1). Given that HIF-1α is a nuclear transcription factor, we also detected the nuclear expression of HIF-1α after surgery and the HIF-1α nucleoprotein was increased significantly from day 7 to day 21 in BCP rats (Fig. 6A). Next, intrathecal administration of IGF-1R antagonist JB-1 (10 μg/10 μl, once per day from day 14 to day 16 after the operation) significantly inhibited the BCP-induced increase of HIF-1α nucleoprotein (Fig. 6B). Meanwhile, we also examined the effect of IGF-1 on HIF-1α in vitro, western blot analysis showed that the expression of HIF-1α was significantly increased after IGF-1 incubation, and the increase in HIF-1α induced by IGF-1 was almost completely blocked in the presence of HIF-1α siRNA (Supplementary Fig. S2). Moreover, the behavioral test revealed that intrathecal application of HIF-1α siRNA (2 μg/10 μl, once per day from day 7 to day 9 after the operation) apparently attenuated mechanical (Fig. 6C) and thermal (Fig. 6D) sensitivity in BCP rats. Taken together, these results suggest that activation of HIF-1α plays an important role in the development of BCP.

To further determine whether IGF-1 signal pathway regulates the Cav3.2 channel through activation of HIF-1α, we examined the impact of HIF-1α on Cav3.2 expression in vivo and in vitro. First, suppression of HIF-1α by siRNA obviously prevented BCP-induced increase of Cav3.2 (Fig. 6E). And the upregulation of Cav3.2 after treatment of IGF-1 in PC12 cells was almost reversed by HIF-1α siRNA (Fig. 6F). Considering that HIF-1α, as a transcription factor, can regulate the transcription of several calcium modulators and lead to the reconstruction of the calcium signaling pathway [16], we next performed an EMSA to determine

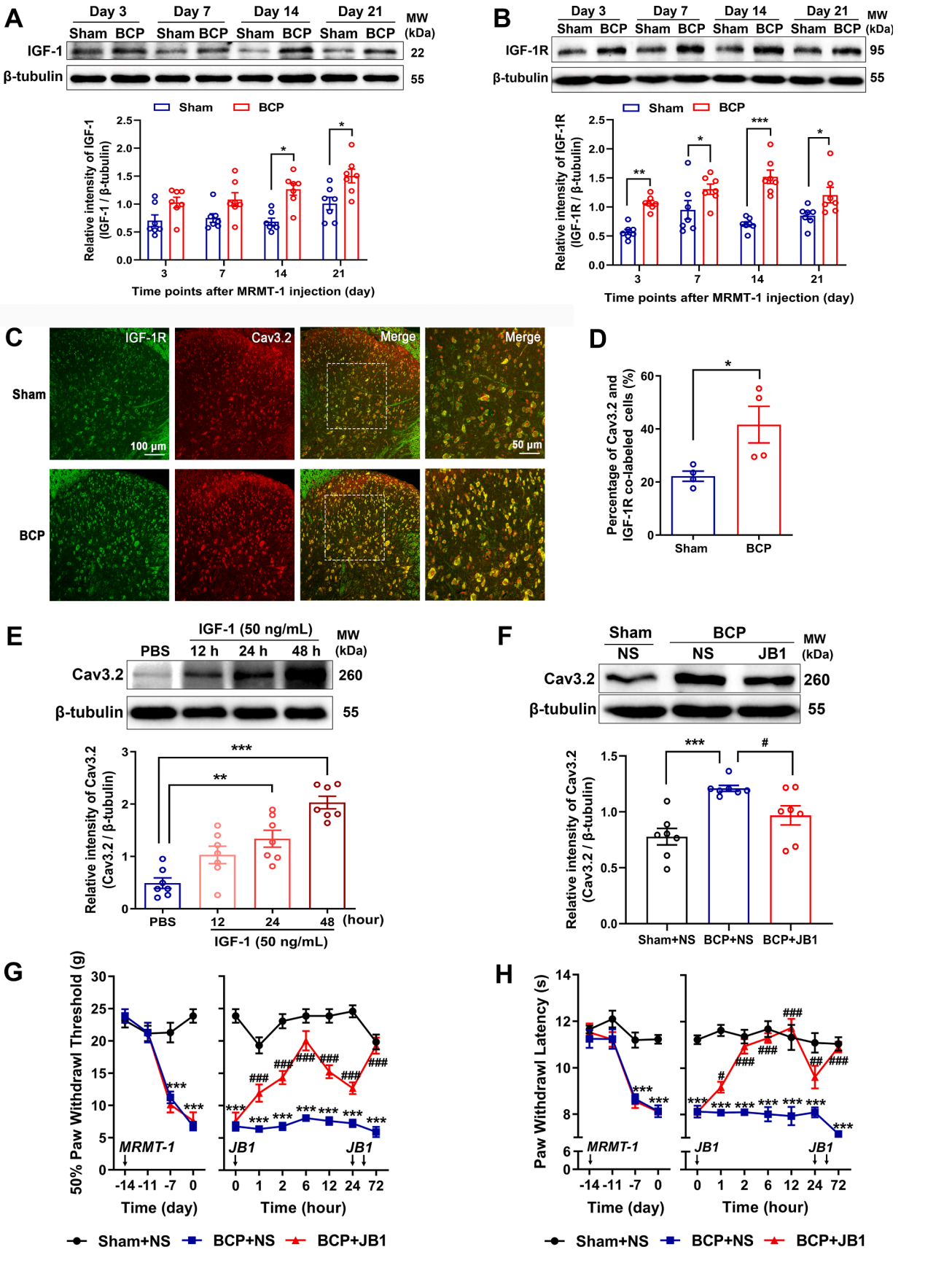

(caption on next page)

Fig. 5. Increased expression of IGF-1 and IGF-1R and inhibition of IGF-1R reverses the upregulation of Cav3.2 and alleviates pain hypersensitivity in BCP rats. (A) IGF-1 expression increased in the dorsal horn of the spinal cord from day 14 to day 21 in BCP rats compared to sham-operation rats. Upper: representative image of Western blot bands in ipsilateral side of the lumbar enlargement lysates; lower: statistical analysis of protein expression. n = 7. $^{*}p < 0.05$, two-way ANOVA with Bonferroni's *post hoc* test. (B) IGF-1R expression increased in the dorsal horn of the spinal cord from day 3 to day 21 in BCP rats compared to sham-operation rats. Upper: representative image of Western blot bands in ipsilateral side of the lumbar enlargement lysates; lower: statistical analysis of protein expression. n = 7. $^{*}p < 0.05$, two-way ANOVA with Bonferroni's *post hoc* test. (C) Representative immunofluorescent images 14 days after BCP and sham rats. (D) Quantification showed that the percentage of Cav3.2 and IGF-1R colabeled cells increased in the BCP group compared to the sham group. Scale bar = 100 or 50 μm (the partial lumbar enlargements). n = 4. $^{*}p < 0.05$, $^{***}p < 0.001$, unpaired *t* test. (E) Incubation of IGF-1 for 24 – 48 h in cultured PC12 cells produced an increase in Cav3.2 protein compared to the PBS treatment group. Upper: representative Western blot bands; lower: statistical analysis of protein expression. n = 7. $^{**}p < 0.01$, $^{***}p < 0.001$, one-way ANOVA with Bonferroni's *post hoc* test. (F) JB-1, an antagonist of IGF-1R, prevented the BCP-stimulated accumulation of Cav3.2 compared to NS treatment rats. $^{***}p < 0.001$, BCP + NS *vs.* Sham + NS; $^{\#}p < 0.05$, BCP + JB-1 *vs.* BCP + NS, unpaired *t* test. (G and H) Three consecutive days of intrathecal application of JB-1 attenuated mechanical allodynia (G) and thermal hyperalgesia (H) 14 days after BCP. n = 8. $^{***}p < 0.001$, BCP + NS *vs.* Sham + NS; $^{\#}p < 0.05$, $^{\#\#}p < 0.01$, $^{\#\#\#}p < 0.001$, BCP + JB-1 *vs.* BCP + NS, two-way ANOVA with Bonferroni's *post hoc* test.

whether HIF-1α bound to the Cav3.2 gene promoter to play roles in BCP rats. As shown in Fig. 6G, a significant increase in the association of HIF-1α nuclear protein with the Cav3.2 binding sequence was observed following BCP (lanes 5–7) compared to the sham group (lanes 2–4). The mutated probe was not bound to HIF-1α to form complexes (lane 8), and these HIF-1α-labeled probe complexes were prevented from competition by unlabeled oligonucleotides (lane 9). The EMSA analysis assay indicated that HIF-1α could bind to the Cav3.2 promoter and positively regulate the Cav3.2 transcription level in BCP rats. These findings suggest that IGF-1 acted as an activator to regulate HIF-1α accumulation by binding to the Cav3.2 promoter directly, providing new information on the regulatory mechanism of bone cancer-induced pain.

4. Discussion

Cancer pain with bone metastasis represents a main clinical, economic and social burdens that impairs almost all ages. Although various methods are currently used for treatment in BCP, at least 45% of cancer pain is still poorly controlled and needs to be improved [28,29]. BCP is associated with a specific pain process that involves a combination of inflammatory and neuropathic pain but unique features [3,30]. In the present study, we demonstrate that activation of Cav3.2 T-type calcium channels in the spinal cord plays an important role in the development of BCP. Numerous studies have shown that Cav3.2 expression and/or activity are significantly increased in the spinal dorsal horn and DRG neurons in various painful modalities, including neuropathic and inflammatory pain [4,31–33]. Moreover, using direct channel blockers [6,34], gene knockdown [35] and genetic tracing [36] methods have demonstrated the importance of Cav3.2 channels in exhibiting potent antihyperalgesic and antiallodynic effects in pain models. However, the possible role of Cav3.2 T-type channels in the spinal cord of BCP rats have not been reported. In pain studies, MRMT-1 mammary gland carcinoma cells were firstly developed by Medhurst et al. to induce bone cancer in rats, which offered a reliable pre-clinical model for studying pain related to bone metastases [18,37,38]. Accordingly, we used MRMT-1 cells to establish a sustained and stable cancer pain model. The degree of disease development was divided into the early (day 7–8 post MRMT-1 cell injection) or late (day 14–16) stage according to bone destruction [39]. Corresponding to time-dependent trabecular bone destruction, 7 days after tumor inoculation, rats showed a significant decrease in the pain threshold that continued until day 21 after surgery.

In the pain pathway, the spinal dorsal horn is a major center for peripheral sensory information integration, and nociception is believed to be influenced to a large extent by the excitability of neurons in the spinal cord [40,41]. This is regulated by a variety of membrane ion channels, including sodium channels [42], potassium channels [43] and calcium channels [44]. Cav3.2 T-type calcium channels, an important member of the voltage-gated calcium channel family, are sensitive to changes in cell membrane potential and allow calcium ions to participate in a variety of life activities. Previous evidence indicates that all three mRNA transcripts of Cav3.1, Cav3.2 and Cav3.3 are present in the spinal dorsal horn, whereas Cav3.2 is mostly located in the superficial dorsal horn and played important functions for nociceptive neurotransmission in lamina II neurons of spinal cord [45]. Moreover, T-type calcium channels are involved in controlling the proliferation, angiogenesis and invasion of tumor cells in a variety of cancers [7], suggesting that Cav3.2 channels may be an ideal therapeutic target for cancer pain, inhibiting both tumor growth and the pain associated with cancer. In this study, our results showed that there was a significant increase in Cav3.2 expression that was highly concentrated in neurons in the spinal cord of BCP rats. This is consistent with studies in neuropathic pain or arthritic pain models [46,47], indicating that hyperexcitability of spinal cord neurons is a major driver of chronic pain symptoms. In addition, we observed that Cav3.2 was also expressed in microglia sparingly. Neuroinflammation in the spinal cord has been considered an essential process in chronic pain [48].

It has been reported that activation of microglial signaling, such as MAPKs, promotes to the facilitation of spinal pain processing via neuron-microglia interactions, and release of microglial mediators stimulates neuronal excitability in the spinal dorsal horn [49,50]. Deepen knowledge of neuro-immune mechanisms for central sensitization has the latent competence to improve strategies for chronic pain in cancer. Moreover, repetitive administration of Cav3.2 siRNA for three days from days 7–9 and days 14–16 postoperatively almost reversed mechanical allodynia and thermal hyperalgesia in BCP rats, providing the first direct evidence that silencing Cav3.2 was effective in alleviating bone cancer-induced pain in rats. However, the electrophysiological functional changes in Cav3.2 channels was not detected and requires further investigation.

In addition, we demonstrate novel evidence proving that IGF-1/IGF-1R signaling plays a critical role in BCP by upregulating Cav3.2 channels at the spinal cord level through activation of HIF-1α. IGF-1 is a widely expressed multipotent neurotrophic factor and contributes to regulate neuroinflammation [9], it can increase Cav3.2 channel currents and further activate the PKCα pathway to involve in inflammatory pain in the dorsal root ganglion [8]. IL-6 was suppressed by IGF-1R antagonism or IGF-1 neutralization in neuropathic pain [51,52], and we have reported that the accumulation of Cav3.2 channel is regulated by IL-6 in rats with neuropathic pain [6]. The biological actions of IGF-1 are mediated by activation of IGF-1R, a transmembrane heterotetramer initiated in the ras-MAPK and PI3K/AKT signal cascade, which controls metabolic and mitogenic outcomes, such as cell growth and differentiations [53,54]. In our study, we found increased colocalization of Cav3.2 and IGF-1R in spinal dorsal horn neurons of BCP rats, which formed the morphological basis for the regulation of Cav3.2 calcium channels by IGF-1/IGF-1R signaling. In the spinal cord, IGF-1 colocalizes with neurons, astrocytes, and microglia, and IGF-1/IGF1R signaling is implicated in reducing microglia-mediated neuroinflammation in painful diabetic neuropathy [55]. IGF-1 might be confined to the bone marrow cavity at the early stage of metastasis and not until the late stage that the bone cortex is destroyed by cancer cells, and increased IGF-1 can reach the nerve fiber endings and induce upregulation of Cav3.2 expression [10]. As the rat pheochromocytoma PC12 cell line was one of the typically utilized neural cell models [56,57], we chose the neuron-

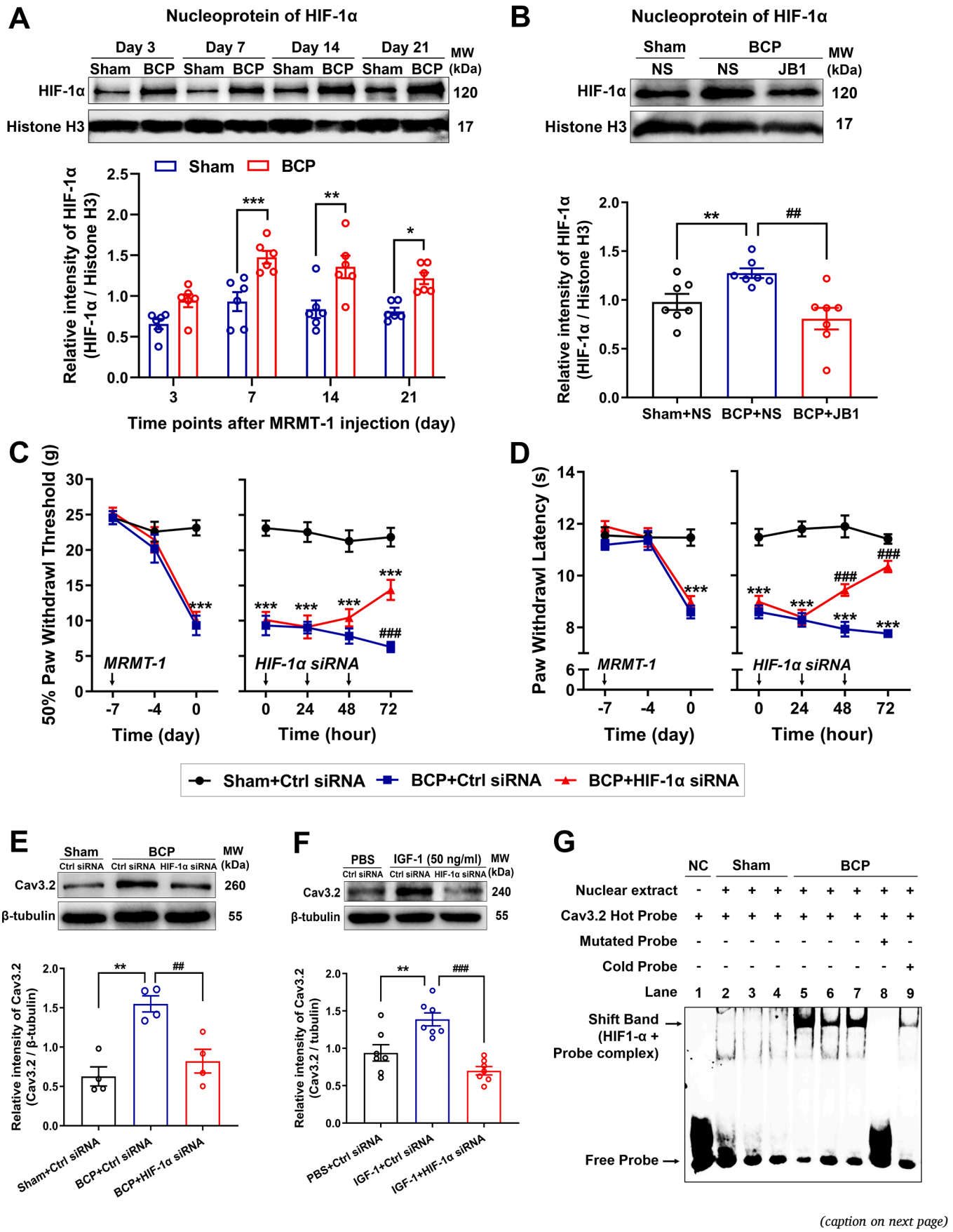

(caption on next page)

Fig. 6. Expression of HIF-1α is increased in BCP rats, and knockdown of HIF-1α prevents upregulation of Cav3.2 induced by IGF-1. (A) Nucleoprotein expression of HIF-1α increased from day 7 to day 21 in BCP rats compared to sham operation rats. Upper: representative image of Western blot bands in ipsilateral side of the lumbar enlargement lysates; lower: statistical analysis of protein expression. n = 6. $^{*}p < 0.05$, $^{**}p < 0.01$, $^{***}p < 0.001$, two-way ANOVA with Bonferroni's *post hoc* test. (B) The IGF-1R inhibitor JB-1 reversed the increase in the expression of HIF-1α nucleoprotein expression in the spinal dorsal horn in BCP rats. $^{**}p < 0.01$, BCP + NS *vs.* Sham + NS; $^{\#\#}p < 0.01$, BCP + JB-1 *vs.* BCP + NS, unpaired *t* test. (C, D) Three consecutive days of intrathecal application of HIF-1α siRNA attenuated mechanical allodynia (C) and thermal hyperalgesia (D) 7 days after BCP. n = 8. $^{***}p < 0.001$, BCP + Ctrl siRNA *vs.* Sham + Ctrl siRNA; $^{\#\#\#}p < 0.001$, BCP + HIF-1α siRNA *vs.* BCP + Ctrl siRNA, two-way ANOVA with Bonferroni's *post hoc* test. (E) Pretreatment with HIF-1α siRNA reversed the increased expression of Cav3.2 induced by IGF-1. n = 6. $^{**}p < 0.01$, BCP + Ctrl siRNA *vs.* Sham + Ctrl siRNA; $^{\#\#\#}p < 0.001$, BCP + HIF-1α siRNA *vs.* BCP + Ctrl siRNA, unpaired *t* test. (F) Pretreatment with HIF-1α siRNA reversed the increased expression of Cav3.2 induced by IGF-1. n = 6. $^{**}p < 0.01$, IGF-1 + Ctrl siRNA *vs.* PBS + Ctrl siRNA; $^{\#\#\#}p < 0.001$, IGF-1 + HIF-1α siRNA *vs.* IGF-1 + Ctrl siRNA, unpaired *t* test. (G) EMSA showed that nucleus HIF-1α bind to the core promoter region of Cav3.2, and these Cav3.2-labeled probe complexes were abrogated by competition from the unlabeled fragments.

like PC12 cells for our experiments in vitro. The results showed that the expression of Cav3.2 was significantly increased after long-term exposure of PC12 cells to IGF-1. To connect the results of in vitro experiments, we observed the effects of the IGF-1R antagonist JB-1 on mechanical and thermal nociception, which were successfully reversed in rats with BCP. Increasing evidence supports that IGF-1 contributes to pain hypersensitivity through its receptor IGF-1R by activating IGF-1R/Akt or MAPK signaling pathways [53,54]. Activation of the Ras-ERK signaling pathway is responsible for enhancing the activity of Cav3.2 channels [58]. The IGF-1/HIF-1α/Cav3.2 signaling pathway involves in the pathogenesis of MRMT-1 induced-BCP in rats, but insufficient evidence to extend to the BCP of other cell lines, such as NCTC2472 sarcoma cells, MLL prostate cancer cells, Lewis lung cancer cells and so on. Further research using multiple cell lines will verify and improve the findings of this study.

The transcription factor HIF-1α plays a pivotal role in tumor proliferation and is regulated through a number of signaling pathways [59,60]. IGF-1 induces Ras and CaMKII to elevate HIF-1α transcriptional activity, and intrathecal administration of JB-1 reversed the increase in HIF-1α induced by BCP [61]. Previous studies have shown that IGF-1/IGF-1R signaling is involved in the ERK1/2 and AKT transduction pathways to induce HIF-1α expression in the tumor microenvironment [13]. The knockdown of Annexin A3 in spinal cord microglia has been reported to reduce the levels of HIF-1α/VEGF and attenuate BCP behavior [62]. Notably, HIF-1α may be dichotomous in nociception. Intermittent hypoxia can reduce pain sensitivity in rats by activating HIF-1α [63]. In this study, pain duality in HIF-1α was not observed. HIF-1α elimination reduced the expression of Cav3.2 channels and attenuated nociceptive sensitization in BCP rats. In in vitro experiments, HIF-1α siRNA successfully reversed the upregulation of Cav3.2 channels after incubation with IGF-1. Under pathological conditions, accumulated HIF-1α in the cytoplasm is transported to the nucleus, where it regulates the transcription of downstream target genes [64]. The EMSA results showed that Cav3.2 probes with characteristic binding to HIF-1α exhibited higher gray values, suggesting that HIF-1α may regulate the transcriptional level of Cav3.2 by binding to the promoter region. In contrast, transcriptional level regulation seems to be a more controllable and acceptable technique. Future efforts should be made to develop small molecules that can manipulate transcriptional level regulation.

In conclusion, our present study suggest that IGF-1 upregulates

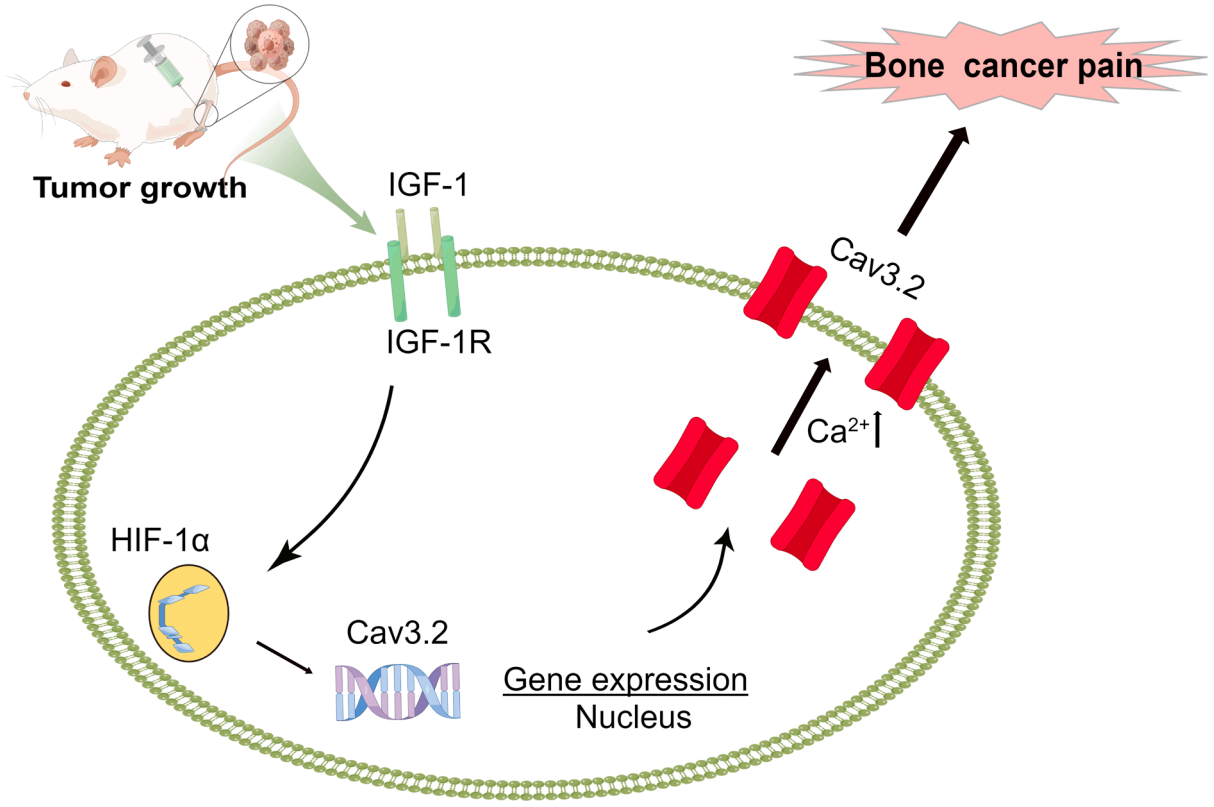

Fig. 7. A schematic of IGF-1-mediated upregulation of Cav3.2 T-type channels through HIF-1α in the spinal dorsal horn during the development of BCP. The expression of IGF-1/IGF-1R and HIF-1α were increased in the spinal dorsal horn after BCP. Elevated IGF-1 bound to IGF-1R, subsequently activated HIF-1α and then triggered upregulation of Cav3.2 T-type channels. Potentiated Cav3.2 T-type channels lead to an increase in calcium influx and result in pain hypersensitivity that is BCP–induced.

Cav3.2 T-type channels expression through the IGF-1/IGF-1R/HIF-1α signaling pathway in spinal dorsal horn, thus contributes to the development of bone cancer-induced pain in rats. In addition, the study proposes a positive regulation of Cav3.2 by HIF-1α at the transcriptional level (Fig. 7). These results may provide a new mechanism in chronic BCP and suggest that Cav3.2 T-type calcium channels can be a novel promising target for the treatment of bone cancer pain.

Funding

This work was supported by the National Natural Science Foundation of China (82001182), the Medical Science and Technology Project of Henan Province (LHGJ20190214), the National Key Research and Development Program of China (2020YFC2008400), and The Science and Technology Project of Henan Province (International Science and Technology Cooperation Field) (182102410014).

Author contribution

QYL, ZYL, JW, WDZ, JC, and XCF designed the experiment. QYL, ZYL, HR, LJF, YLW, HLB, LTM and CH performed the experiments. QYL, ZYL, MYM, WDZ, and JC analyzed the data. QYL, ZYL, and XCF wrote the manuscript.

7. Consent for publication

All authors have read and approved the submission of the manuscript.

Data availability

All data needed to evaluate the conclusions in the paper are present in the paper and/or the Supplementary Materials. Additional data related to this paper may be requested from the authors.

9. Ethics approval

All experimental procedures for animals were approved by the Animal Protection and Use Committee of Zhengzhou University.

Declaration of Competing Interest

The authors declare that they have no known competing financial interests or personal relationships that could have appeared to influence the work reported in this paper.

Acknowledgment

The images in this article were drawn by Figdraw.

Appendix A. Supplementary data

Supplementary data to this article can be found online at https://doi.org/10.1016/j.jbo.2023.100495.

References

[1] K.N. Weilbaecher, T.A. Guise, L.K. McCauley, Cancer to bone: a fatal attraction, Nat. Rev. Cancer 11 (6) (2011) 411–425, https://doi.org/10.1038/nrc3055.
[2] L. Feller, R.A.G. Khammissa, M. Bouckaert, R. Ballyram, Y. Jadwat, J. Lemmer, Pain: Persistent postsurgery and bone cancer-related pain, J. Int. Med. Res. 47 (2) (2019) 528–543, https://doi.org/10.1177/0300060518818296.
[3] S. Falk, A.H. Dickenson, Pain and nociception: mechanisms of cancer-induced bone pain, J. Clin. Oncol. 32 (16) (2014) 1647–1654, https://doi.org/10.1200/JCO.2013.51.7219.
[4] S. Cai, K. Gomez, A. Moutal, R. Khanna, Targeting T-type/CaV3.2 channels for chronic pain, Transl. Res. 234 (2021) 20–30, https://doi.org/10.1016/j.trsl.2021.01.002.
[5] P.M. Kamau, H. Li, Z. Yao, Y. Han, A. Luo, H. Zhang, C. Boonyarat, C. Yenjai, J. Mwangi, L. Zeng, S. Yang, R. Lai, L. Luo, Potent Ca(V)3.2 channel inhibitors exert analgesic effects in acute and chronic pain models, Biomed Pharmacother 153 (2022) 113310, 10.1016/j.biopha.2022.113310.
[6] Q. Liu, W. Chen, X. Fan, J. Wang, S. Fu, S. Cui, F. Liao, J. Cai, X. Wang, Y. Huang, L. Su, L. Zhong, M. Yi, F. Liu, Y. Wan, Upregulation of interleukin-6 on Cav3.2 T-type calcium channels in dorsal root ganglion neurons contributes to neuropathic pain in rats with spinal nerve ligation, Exp. Neurol. 317 (2019) 226–243, https://doi.org/10.1016/j.expneurol.2019.03.005.
[7] G. Santoni, M. Santoni, M. Nabissi, Functional role of T-type calcium channels in tumour growth and progression: prospective in cancer therapy, Br. J. Pharmacol. 166 (4) (2012) 1244–1246, https://doi.org/10.1111/j.1476-5381.2012.01908.x.
[8] Y. Zhang, W. Qin, Z. Qian, X. Liu, H. Wang, S. Gong, Y.G. Sun, T.P. Snutch, X. Jiang, J. Tao, Peripheral pain is enhanced by insulin-like growth factor 1 through a G protein-mediated stimulation of T-type calcium channels, Sci. Signal. 7 (346) (2014) ra94, DOI: 10.1126/scisignal.2005283.
[9] R. Baserga, A. Hongo, M. Rubini, M. Prisco, B. Valentinis, The IGF-I receptor in cell growth, transformation and apoptosis, BBA 1332 (3) (1997) F105–F126, https://doi.org/10.1016/s0304-419x(97)00007-3.
[10] Y. Li, J. Cai, Y. Han, X. Xiao, X.L. Meng, L. Su, F.Y. Liu, G.G. Xing, Y. Wan, Enhanced function of TRPV1 via up-regulation by insulin-like growth factor-1 in a rat model of bone cancer pain, Eur. J. Pain 18 (6) (2014) 774–784, https://doi.org/10.1002/j.1532-2149.2013.00420.x.
[11] P. Stemkowski, A. Garcia-Caballero, V.M. Gadotti, S. M'Dahoma, S. Huang, S.A. G. Black, L. Chen, I.A. Souza, Z. Zhang, G.W. Zamponi, TRPV1 Nociceptor Activity Initiates USP5/T-type Channel-Mediated Plasticity, Cell Rep. 17 (11) (2016) 2901–2912, https://doi.org/10.1016/j.celrep.2016.11.047.
[12] L. You, W. Wu, X. Wang, L. Fang, V. Adam, E. Nepovimova, Q. Wu, K. Kuca, The role of hypoxia-inducible factor 1 in tumor immune evasion, Med. Res. Rev. 41 (3) (2021) 1622–1643, https://doi.org/10.1002/med.21771.
[13] E.M. De Francesco, A.H. Sims, M. Maggiolini, F. Sotgia, M.P. Lisanti, R.B. Clarke, GPER mediates the angiocrine actions induced by IGF1 through the HIF-1alpha/VEGF pathway in the breast tumor microenvironment, Breast Cancer Res. 19 (1) (2017) 129, https://doi.org/10.1186/s13058-017-0923-5.
[14] H.L. Lee, H.Y. Lee, Y. Yun, J. Oh, L. Che, M. Lee, Y. Ha, Hypoxia-specific, VEGF-expressing neural stem cell therapy for safe and effective treatment of neuropathic pain, J. Control. Release 226 (2016) 21–34, https://doi.org/10.1016/j.jconrel.2016.01.047.
[15] D. Selvaraj, V. Gangadharan, C.W. Michalski, M. Kurejova, S. Stosser, K. Srivastava, M. Schweizerhof, J. Waltenberger, N. Ferrara, P. Heppenstall, M. Shibuya, H. G. Augustin, R. Kuner, A functional role for VEGFR1 expressed in peripheral sensory neurons in cancer pain, Cancer Cell 27 (6) (2015) 780–796, https://doi.org/10.1016/j.ccell.2015.04.017.
[16] I. Azimi, The interplay between HIF-1 and calcium signalling in cancer, Int. J. Biochem. Cell Biol. 97 (2018) 73–77, https://doi.org/10.1016/j.biocel.2018.02.001.
[17] V.V. Makarenko, G.U. Ahmmed, Y.J. Peng, S.A. Khan, J. Nanduri, G.K. Kumar, A. P. Fox, N.R. Prabhakar, CaV3.2 T-type Ca2+ channels mediate the augmented calcium influx in carotid body glomus cells by chronic intermittent hypoxia, J. Neurophysiol. 115 (1) (2016) 345–354, https://doi.org/10.1152/jn.00775.2015.
[18] Y. Yang, S. Li, Z.R. Jin, H.B. Jing, H.Y. Zhao, B.H. Liu, Y.J. Liang, L.Y. Liu, J. Cai, Y. Wan, G.G. Xing, Decreased abundance of TRESK two-pore domain potassium channels in sensory neurons underlies the pain associated with bone metastasis, Sci. Signal. 11 (552) (2018), https://doi.org/10.1126/scisignal.aao5150.
[19] S.R. Chaplan, F.W. Bach, J.W. Pogrel, J.M. Chung, T.L. Yaksh, Quantitative assessment of tactile allodynia in the rat paw, J. Neurosci. Methods 53 (1) (1994) 55–63, https://doi.org/10.1016/0165-0270(94)90144-9.
[20] J.Y. Zhao, L. Liang, X. Gu, Z. Li, S. Wu, L. Sun, F.E. Atianjoh, J. Feng, K. Mo, S. Jia, B.M. Lutz, A. Bekker, E.J. Nestler, Y.X. Tao, DNA methyltransferase DNMT3a contributes to neuropathic pain by repressing Kcna2 in primary afferent neurons, Nat. Commun. 8 (2017) 14712, https://doi.org/10.1038/ncomms14712.
[21] J. Zheng, Y.Y. Jiang, L.C. Xu, L.Y. Ma, F.Y. Liu, S. Cui, J. Cai, F.F. Liao, Y. Wan, M. Yi, Adult hippocampal neurogenesis along the dorsoventral axis contributes differentially to environmental enrichment combined with voluntary exercise in alleviating chronic inflammatory pain in mice, J. Neurosci. 37 (15) (2017) 4145–4157, https://doi.org/10.1523/JNEUROSCI.3333-16.2017.
[22] Y.Y. Jiang, S. Shao, Y. Zhang, J. Zheng, X. Chen, S. Cui, F.Y. Liu, Y. Wan, M. Yi, Neural pathways in medial septal cholinergic modulation of chronic pain: distinct contribution of the anterior cingulate cortex and ventral hippocampus, Pain 159 (8) (2018) 1550–1561, https://doi.org/10.1097/j.pain.0000000000001240.
[23] Q.Y. Liu, W. Chen, S. Cui, F.F. Liao, M. Yi, F.Y. Liu, Y. Wan, Upregulation of Cav3.2 T-type calcium channels in adjacent intact L4 dorsal root ganglion neurons in neuropathic pain rats with L5 spinal nerve ligation, Neurosci. Res. 142 (2019) 30–37, https://doi.org/10.1016/j.neures.2018.04.002.
[24] Z. Li, Y. Guo, X. Ren, L. Rong, M. Huang, J. Cao, W. Zang, HDAC2, but not HDAC1, regulates Kv1.2 expression to mediate neuropathic pain in CCI rats, Neuroscience 408 (2019) 339–348, https://doi.org/10.1016/j.neuroscience.2019.03.033.
[25] Z. Pietrzkowski, D. Wernicke, P. Porcu, B.A. Jameson, R. Baserga, Inhibition of cellular proliferation by peptide analogues of insulin-like growth factor 1, Cancer Res. 52 (23) (1992) 6447–6451.
[26] A.R. Sartori-Cintra, C.S. Mara, D.L. Argolo, I.B. Coimbra, Regulation of hypoxia-inducible factor-1alpha (HIF-1alpha) expression by interleukin-1beta (IL-1 beta), insulin-like growth factors I (IGF-I) and II (IGF-II) in human osteoarthritic chondrocytes, Clinics (Sao Paulo) 67 (1) (2012) 35–40, https://doi.org/10.6061/clinics/2012(01)06.

[27] N. Baran, M. Konopleva, Molecular Pathways: Hypoxia-activated prodrugs in cancer therapy, Clin. Cancer Res. 23 (10) (2017) 2382–2390, https://doi.org/10.1158/1078-0432.CCR-16-0895.
[28] P.W. Mantyh, D.R. Clohisy, M. Koltzenburg, S.P. Hunt, Molecular mechanisms of cancer pain, Nat. Rev. Cancer 2 (3) (2002) 201–209, https://doi.org/10.1038/nrc747.
[29] M.H. van den Beuken-van Everdingen, L.M. Hochstenbach, E.A. Joosten, V.C. Tjan-Heijnen, D.J. Janssen, Update on prevalence of pain in patients with cancer: systematic review and meta-analysis, J Pain Symptom Manage 51(6) (2016) 1070-1090 e9, 10.1016/j.jpainsymman.2015.12.340.
[30] C.M. Kane, P. Hoskin, M.I. Bennett, Cancer induced bone pain, BMJ 350 (2015), h315, https://doi.org/10.1136/bmj.h315.
[31] E.K. Harding, G.W. Zamponi, Central and peripheral contributions of T-type calcium channels in pain, Mol. Brain 15 (1) (2022) 39, https://doi.org/10.1186/s13041-022-00923-w.
[32] T.P. Snutch, G.W. Zamponi, Recent advances in the development of T-type calcium channel blockers for pain intervention, Br. J. Pharmacol. 175 (12) (2018) 2375–2383, https://doi.org/10.1111/bph.13906.
[33] T. Takahashi, Y. Aoki, K. Okubo, Y. Maeda, F. Sekiguchi, K. Mitani, H. Nishikawa, A. Kawabata, Upregulation of Ca(v)3.2 T-type calcium channels targeted by endogenous hydrogen sulfide contributes to maintenance of neuropathic pain, Pain 150 (1) (2010) 183–191, https://doi.org/10.1016/j.pain.2010.04.022.
[34] S.L. Joksimovic, S.M. Joksimovic, V. Tesic, A. Garcia-Caballero, S. Feseha, G. W. Zamponi, V. Jevtovic-Todorovic, S.M. Todorovic, Selective inhibition of Ca(V) 3.2 channels reverses hyperexcitability of peripheral nociceptors and alleviates postsurgical pain, Sci. Signal. 11 (545) (2018), https://doi.org/10.1126/scisignal.aao4425.
[35] E. Bourinet, A. Alloui, A. Monteil, C. Barrere, B. Couette, O. Poirot, A. Pages, J. McRory, T.P. Snutch, A. Eschalier, J. Nargeot, Silencing of the Cav3.2 T-type calcium channel gene in sensory neurons demonstrates its major role in nociception, EMBO J. 24 (2) (2005) 315–324, https://doi.org/10.1038/sj.emboj.7600515.
[36] Y.A. Bernal Sierra, J. Haseleu, A. Kozlenkov, V. Begay, G.R. Lewin, Genetic Tracing of Ca(v)3.2 T-Type calcium channel expression in the peripheral nervous system, Front. Mol. Neurosci. 10 (2017), https://doi.org/10.3389/fnmol.2017.00070, 70.
[37] S.J. Medhurst, K. Walker, M. Bowes, B.L. Kidd, M. Glatt, M. Muller, M. Hattenberger, J. Vaxelaire, T. O'Reilly, G. Wotherspoon, J. Winter, J. Green, L. Urban, A rat model of bone cancer pain, Pain 96 (1–2) (2002) 129–140, https://doi.org/10.1016/s0304-3959(01)00437-7.
[38] Y. Chen, J. Luan, T. Jiang, D. Cai, C. Sun, X. Wang, X. Zhao, X. Gou, Knockdown of EMMPRIN (OX47) in MRMT-1 carcinoma cells inhibits tumor growth and decreases cancer-induced bone destruction and pain, Cancer Res. Treat. 53 (2) (2021) 576–583, https://doi.org/10.4143/crt.2020.801.
[39] M.W. Kucharczyk, D. Derrien, A.H. Dickenson, K. Bannister, The stage-specific plasticity of descending modulatory controls in a rodent model of cancer-induced bone pain, Cancers (Basel) 12 (11) (2020), https://doi.org/10.3390/cancers12113286.
[40] F. Moehring, P. Halder, R.P. Seal, C.L. Stucky, Uncovering the cells and circuits of touch in normal and pathological settings, Neuron 100 (2) (2018) 349–360, https://doi.org/10.1016/j.neuron.2018.10.019.
[41] C. Peirs, R.P. Seal, Neural circuits for pain: Recent advances and current views, Science 354 (6312) (2016) 578–584, https://doi.org/10.1126/science.aaf8933.
[42] S. Su, J. Shao, Q. Zhao, X. Ren, W. Cai, L. Li, Q. Bai, X. Chen, B. Xu, J. Wang, J. Cao, W. Zang, MiR-30b Attenuates neuropathic pain by regulating voltage-gated sodium channel Nav1.3 in rats, Front Mol Neurosci 10 (2017) 126, 10.3389/fnmol.2017.00126.
[43] F. Fan, Y. Chen, Z. Chen, L. Guan, Z. Ye, Y. Tang, A. Chen, C. Lin, Blockade of BK channels attenuates chronic visceral hypersensitivity in an IBS-like rat model, Mol Pain 17 (2021) 17448069211040364, 10.1177/17448069211040364.
[44] Z. Cai, L. Quan, X. Chang, Z. Qiu, H. Zhou, High-voltage long-duration pulsed radiofrequency attenuates neuropathic pain in CCI rats by inhibiting Cav2.2 in spinal dorsal horn and dorsal root ganglion, Brain Res 1785 (2022) 147892, 10.1016/j.brainres.2022.147892.
[45] M. Candelas, A. Reynders, M. Arango-Lievano, C. Neumayer, A. Fruquiere, E. Demes, J. Hamid, C. Lemmers, C. Bernat, A. Monteil, V. Compan, S. Laffray, P. Inquimbert, Y. Le Feuvre, G.W. Zamponi, A. Moqrich, E. Bourinet, P.F. Mery, Cav3.2 T-type calcium channels shape electrical firing in mouse Lamina II neurons, Sci Rep 9(1) (2019) 3112, 10.1038/s41598-019-39703-3.
[46] X.J. Feng, L.X. Ma, C. Jiao, H.X. Kuang, F. Zeng, X.Y. Zhou, X.E. Cheng, M.Y. Zhu, D.Y. Zhang, C.Y. Jiang, T. Liu, Nerve injury elevates functional Cav3.2 channels in superficial spinal dorsal horn, Mol Pain 15 (2019) 1744806919836569, 10.1177/1744806919836569.
[47] S.M. Shin, Y. Cai, B. Itson-Zoske, C. Qiu, X. Hao, H. Xiang, Q.H. Hogan, H. Yu, Enhanced T-type calcium channel 3.2 activity in sensory neurons contributes to neuropathic-like pain of monosodium iodoacetate-induced knee osteoarthritis, Mol Pain 16 (2020) 1744806920963807, 10.1177/1744806920963807.
[48] L. Teixeira-Santos, A. Albino-Teixeira, D. Pinho, Neuroinflammation, oxidative stress and their interplay in neuropathic pain: Focus on specialized pro-resolving mediators and NADPH oxidase inhibitors as potential therapeutic strategies, Pharmacol. Res. 162 (2020), 105280, https://doi.org/10.1016/j.phrs.2020.105280.
[49] R.R. Ji, T. Berta, M. Nedergaard, Glia and pain: is chronic pain a gliopathy?, Pain 154 Suppl 1(0 1) (2013) S10-S28, 10.1016/j.pain.2013.06.022.
[50] I.H.T. Ho, M.T.V. Chan, W.K.K. Wu, X. Liu, Spinal microglia-neuron interactions in chronic pain, J Leukoc Biol 108(5) (2020) 1575-1592, 10.1002/JLB.3MR0520-695R.
[51] J.L. Labandeira-Garcia, M.A. Costa-Besada, C.M. Labandeira, B. Villar-Cheda, A. I. Rodriguez-Perez, Insulin-like growth factor-1 and neuroinflammation, Front. Aging Neurosci. 9 (2017) 365, https://doi.org/10.3389/fnagi.2017.00365.
[52] X. Chen, Y. Le, W.Y. He, J. He, Y.H. Wang, L. Zhang, Q.M. Xiong, X.Q. Zheng, K. X. Liu, H.B. Wang, Abnormal insulin-like growth factor 1 signaling regulates neuropathic pain by mediating the mechanistic target of rapamycin-related autophagy and neuroinflammation in mice, ACS Chem. Nerosci. 12 (15) (2021) 2917–2928, https://doi.org/10.1021/acschemneuro.1c00271.
[53] H. Werner, D. Le Roith, The insulin-like growth factor-I receptor signaling pathways are important for tumorigenesis and inhibition of apoptosis, Crit. Rev. Oncog. 8 (1) (1997) 71–92, https://doi.org/10.1615/critrevoncog.v8.i1.40.
[54] R. Pfaffle, W. Kiess, J. Klammt, Downstream insulin-like growth factor, Endocr. Dev. 23 (2012) 42–51, https://doi.org/10.1159/000341745.
[55] X. Chen, Y. Le, S.Q. Tang, W.Y. He, J. He, Y.H. Wang, H.B. Wang, Painful diabetic neuropathy is associated with compromised microglial igf-1 signaling which can be rescued by green tea polyphenol EGCG in mice, Oxid. Med. Cell. Longev. 2022 (2022) 6773662, https://doi.org/10.1155/2022/6773662.
[56] A. Jauhari, T. Singh, P. Singh, D. Parmar, S. Yadav, Regulation of miR-34 Family in neuronal development, Mol. Neurobiol. 55 (2) (2018) 936–945, https://doi.org/10.1007/s12035-016-0359-4.
[57] M.R. Cui, W. Zhao, X.L. Li, C.H. Xu, J.J. Xu, H.Y. Chen, Simultaneous monitoring of action potentials and neurotransmitter release from neuron-like PC12 cells, Anal. Chim. Acta 1105 (2020) 74–81, https://doi.org/10.1016/j.aca.2019.11.074.
[58] M. Mor, O. Beharier, S. Levy, J. Kahn, S. Dror, D. Blumenthal, L.A. Gheber, A. Peretz, A. Katz, A. Moran, Y. Etzion, ZnT-1 enhances the activity and surface expression of T-type calcium channels through activation of Ras-ERK signaling, Am. J. Physiol. Cell Physiol. 303 (2) (2012) C192–C203, https://doi.org/10.1152/ajpcell.00427.2011.
[59] K. Balamurugan, HIF-1 at the crossroads of hypoxia, inflammation, and cancer, Int. J. Cancer 138 (5) (2016) 1058–1066, https://doi.org/10.1002/ijc.29519.
[60] L. Ji, W. Shen, F. Zhang, J. Qian, J. Jiang, L. Weng, J. Tan, L. Li, Y. Chen, H. Cheng, D. Sun, Worenine reverses the Warburg effect and inhibits colon cancer cell growth by negatively regulating HIF-1alpha, Cell. Mol. Biol. Lett. 26 (1) (2021) 19, https://doi.org/10.1186/s11658-021-00263-y.
[61] S. Sinha, N. Koul, D. Dixit, V. Sharma, E. Sen, IGF-1 induced HIF-1alpha-TLR9 cross talk regulates inflammatory responses in glioma, Cell. Signal. 23 (11) (2011) 1869–1875, https://doi.org/10.1016/j.cellsig.2011.06.024.
[62] Z. Zhang, M. Deng, J. Huang, J. Wu, Z. Li, M. Xing, J. Wang, Q. Guo, W. Zou, Microglial annexin A3 downregulation alleviates bone cancer-induced pain through inhibiting the Hif-1alpha/vascular endothelial growth factor signaling pathway, Pain 161 (12) (2020) 2750–2762, https://doi.org/10.1097/j.pain.0000000000001962.
[63] J. Wu, P. Li, X. Wu, W. Chen, Chronic intermittent hypoxia decreases pain sensitivity and increases the expression of HIF1alpha and opioid receptors in experimental rats, Sleep Breath. 19 (2) (2015) 561–568, https://doi.org/10.1007/s11325-014-1047-0.
[64] F. Paredes, H.C. Williams, A. San Martin, Metabolic adaptation in hypoxia and cancer, Cancer Lett. 502 (2021) 133–142.